Moisture-induced autonomous surface potential oscillations for energy harvesting

Yu Long
University of California Berkeley

Peisheng He
University of California Berkeley

Zhichun Shao
University of California Berkeley

Han Kim
University of California Berkeley

Archie Yao
Tsinghua University   https://orcid.org/0000-0001-6369-129X

Yande Peng
University of California Berkeley

Renxiao Xu
University of California, Berkeley

Seung-Wuk Lee
University of California, Berkeley

Junwen Zhong (✉ junwenzhong@um.edu.mo)
University of Macau

Liwei Lin
Mechanical Engineering, University of California Berkeley

Abstract

A variety of autonomous oscillations in nature such as heartbeats and biochemical reactions have been widely studied and utilized for applications in the fields of bioscience and energy technology, etc. Here, we report a unique phenomenon of moisture-induced electrical potential oscillations on P(MEDSAH-co-AA) polymers during the diffusion of water molecules. Using the moisture in the ambient environment as the activation source, this self-excited chemoelectrical reaction could have broad influences and usages in surface-reaction based devices and systems. As a proof-of-concept demonstration, an energy harvester is constructed to demonstrate the continuous energy production for more than 15000 seconds with an energy density of 16.8 mJ/cm2. A 2-Volts output voltage has been produced to power a liquid crystal display (LCD) with five energy harvesters connected in series toward practical applications.

Introduction

Electricity has become indispensable in the modern life and many devices have been powered by the electricity delivered from power plants and batteries have been the key energy sources for portable devices.[1] Green energy resources could be the potential substitutes for batteries, such as solar cells powered by the Sun[2,3], and piezoelectric/triboelectric energy generators powered by the ambient vibrations,[4,5] ... *etc.*. A new class of energy source has been demonstrated in recent years with the moisture-electric effects to generate electrical energy based on the proton transportations[6−15], ion transportations[16−18], electrokinetic[19−22] and so on. Specifically, the basic mechanism for moist-electric generators is based on the proton transportation to release protons from the material as the moisture migrates. The operation time under a typical moisture excitation, or the energy generation time in one hydration/dehydration cycle, is an important parameter[22]. However, the humidity level doesn't change quickly in real environments such that the energy outputs of all previously demonstrated devices are restricted. One approach is to limit the diffusion speed of protons in materials[15,23] in order to enhance the device operation time as reported previously. Herein, we report a very different approach with the new phenomenon of self-excited proton concentration oscillations to limit the diffusion process in a carefully designed material system. This drastically improves the operation period and electrical outputs of the moist-electric generator.

On the other hand, forced oscillation is a phenomenon that various and repeated actions can be induced by frequently changed external stimulations, such as forces, temperature, light, or alternating electricity (AC) inputs, *etc.*[24−28] Autonomous oscillations or "self-oscillating" behaviors are continuously changing activities that don't require repeated switching by the external stimulations.[29−33] In nature, autonomous oscillations widely exist in living organisms, such as heartbeats, brain waves, and biochemical reactions[31]. Mimicking and applying various kinds of autonomous oscillations in artificial and practical systems have attracted great interests. For example, prior efforts have applied the periodically swelling and de-swelling process caused by the moisture diffusion process by sunlight as polymeric actuators.[34]

Other polymer-based autonomous oscillations have also been demonstrated for applications in artificial muscles, drug deliveries, and biosensors, ... *etc.*[34−38]

Here, bio-inspired by the autonomous oscillations in nature, autonomous electrical potential oscillations induced by the moisture diffusion process in P(MEDSAH-co-AA) is studied. It is found that the surface electrical potential oscillates continuously to result in alternating current (AC) electrical outputs – very different from the previously reported mechanism of direct current (DC) induced electricity outputs by moistures.[15] Experimentally, a porotype energy harvester has been constructed to utilize the autonomous oscillation mechanism to generate an open-circuit voltage and short-circuit current density of 0.4 V and 2.8 μA/cm^2, respectively. The operation time under one moisture excitation reaches 15000 seconds, with an energy density of 16.8 mJ/cm^2. The voltage output can be further increased to 2 Volts by connecting five devices in series to light up an LCD in a bathroom.

Results And Discussion

Surface potential oscillation

One common oscillation example in nature is the concentration of the Calcium in living cells to assist the transmission of intracellular biological information.[39,40] The Calcium-induced Ca^{2+} release (CICR) process is illustrated in Fig. 1a, where the inositol trisphosphate (IP$_3$) helps releasing Ca^{2+} into the cytoplasm from one pool, leading to an increase in Ca^{2+} concentration. Part of the released Ca^{2+} ions are pumped back to the original pool (1st pool) and another Ca^{2+} pool (2nd pool) also exists in the cytoplasm to release or absorb Ca^{2+} in response to the concentration of the free Ca^{2+}. As a result, the Ca^{2+} concentration oscillates continuously.

The surface potential oscillation observed in this work has a similar phenomenon to the oscillation of the Ca^{2+} concentration in living cells. P(MEDSAH-co-AA) polymer is utilized as the functional material synthesized by a free-radical polymerization method[41]. Two monomers, the [2-(methacryloyloxy)ethyl]dimethyl-(3-sulfopropyl) ammonium hydroxide (MEDSAH) and acrylic acid (AA), are initiated by the ammonium persulfate (APS) and polymerized to form the P(MEDSAH-co-AA) polymer and the detailed process is shown in **Fig. S1a**. The ratios of MEDSAH and AA monomers (MEDSAH/AA) are 1/2, 1/3, and 1/4, respectively, in prototype tests. To characterize monomer distributions inside the polymer, energy-dispersive X-ray (EDX) spectroscopy is performed and the N-Kα line is chosen to represent MEDSAH. **Fig. S2** demonstrates that the two monomers distribute homogeneously in the prototypes of varying MEDSAH/AA ratios. The synthesized polymer is transparent (**Fig. S1b**) and it contains N$^+$, -SO$_3^-$, and -COOH groups (Fig. 1b), which play key roles in the surface potential oscillation process.

The observed surface potential oscillations of the synthesized polymer come from the releasing and capturing process of proton (H$^+$) between the functional groups, as illustrated in Fig. 1c, which is similar

to that of the Calcium oscillations process in living cells. A kinetic model is established with simulation results to calculate the proton concentration outputs as shown in Figs. 1d and 1e. It is found the proton concentration oscillates at about 70 seconds per cycle, and the relative intensity of the proton decreases gradually, which is similar to the Calcium oscillation cycles in living cells.[40] Specifically, it is found that the surface proton intensity decreases to around 87% of its original value after 2000 seconds for a prototype device in simulations with details in **Supporting Explanation 1**.

Figure 2a shows a model schematic diagram of the electrochemical oscillation process with related chemical reactions from r1 to r5. The model starts with the release of protons upon the introduction of moisture, which activates the functional groups in the polymer as evidenced from the Attenuated Total Reflectance Fourier-transform infrared (ATR-FT-IR) spectroscopy (**Fig. S3**). The carboxylic acid (-COOH) groups generate free protons upon the exposure to moisture (r1), which increases the polarity and attracts more moistures to accelerate the ionization process. As a result, the free proton concentration increases in this positive feedback process. Moistures also helps breaking the dynamic bonds between N^+ and -SO_3^- groups (r2), and the SO_3^- groups can capture protons (r3) to form the sulfonic acid (-SO_3H). These two processes are responsible for the decrease of the proton concentration as the negative feedback process. Furthermore, protons are transported from the sulfonic acid to the carboxylic acid and form -COOH (r4) and the dynamic bonds between N^+ and -SO_3^- groups will re-formulate (r5). The overall processes from r1 to r5 (**Fig. S4**) show that N^+, -SO_3^-, and -COOH groups complete their individual cycles as moistures diffuse into the P(MEDSAH-co-AA) polymer to assist this very unique and self-sustainable proton concentration oscillation phenomenon, which results in the surface electrical potential oscillation. This proton oscillation process can be compared with the Ca^{2+} oscillation process in living cells as described in **Supporting Explanation 2**. For instance, IP_3 plays a role similar to H_2O to start the oscillation process; the 1st pool and -COOH groups can execute the positive feedback part of the oscillation procedure, and the 2nd pool and -SO_3^- groups play the role to complete the negative feedback part of the oscillation process.

After saturating the P(MEDSAH-co-AA) polymer with water at 41 wt% (**Fig. S5a**), the Kelvin probe force microscopy (KPFM) is used to measure the surface potential at a fixed area of 500 × 500 nm^2 as depicted in Figs. 2b-e. In general, the average surface potential is found to gradually decrease over time as the moisture evaporates (**Fig. S5b**). However, the time-varying oscillations in a short period of time are also observed. For example, in the white elliptical area in Fig. 2b, the surface potential is found to oscillate during a period of every 12 minutes (this test is limited by the scanning speed of the KPFM) from 0.92 V, 0.85 V, 0.96 V, to 0.74 V, sequentially. This result supports the proposed model and validate simulation results for the surface potential oscillations. The other areas also experience similar but different surface potential oscillations as observed. The surface potentials in the scanning photos in Fig. 2b have shown non-uniform local distributions which are expected due to measurement errors, local structural/chemical variations, and the KPFM scanning sequence (12 minutes for one plot) as the surface potential oscillates.

Application Of Surface Potential Oscillations

The moisture-induced surface potential oscillation is useful for the energy harvesting. Previously, several reports have shown moisture-enabled energy harvesters with DC (direct current) outputs[42−45]. In order to generate the AC (alternating current) outputs, the external moisture concentration level has to be changed actively. This work demonstrates moisture-induced AC power outputs under a relatively constant moisture level. Figure 3a shows the top view optical photo of a prototype energy harvester made of MEDSAH/AA with a ratio of 1/2 and 2 × 2 cm^2 in size. The device has one synthesized P(MEDSAH-co-AA) layer sandwiched by two electrodes made Au coated on a Polyimide (PI) film and the cross-sectional view is shown in **Fig. S6**. The top electrode has circular holes of 2 mm in diameter to allow the direct exposure to moistures.

The surface potential oscillations on the polymer film can induce the electrostatic potential oscillations on the top electrode, which results in AC outputs as demonstrated in COMSOL simulation results in Fig. 3b and **Movie S1**. The electrostatic stationary simulation is implemented here to illustrate electrostatic potential outputs induced by the oscillation of the surface charges.

Experimentally, a specimen has been dried at 30% RH for 24 hours before a wetting process via an ultrasonic humidifier (Pure Enrichment Inc.). Experimental results show electricity generations in the form of AC outputs after the introduction of 100% RH moisture at 1400 seconds by the humidifier. It is found the current density increases initially to a maximum peak value of 2 μA/cm^2 at 2000 seconds (upper left inset in Fig. 3c). The average oscillation period is about 72 seconds, which corresponds well with the kinetic simulation results at 70 seconds (**Fig. S7** and Fig. 1e). The background noise is observed under an average period of about 150 seconds. It is also observed that the current density of the outputs decreases gradually after reaching the peak value. As the humidifier is turned off at 4500 seconds, the system experiences a natural dehydration process and the output current density decreases slowly (upper right insert in Fig. 3c). At around 13,600 seconds, a sudden current density drop is observed to the noise level. In the endurance test under the 100% RH moisture, this energy generation process can last for a very long period from around 500 seconds to 15,000 seconds or about 4 hours as shown in **Fig. S8** before dropping down to the noise level.

Material systems without the key chemical reactions to assist the cyclic process won't be able to induce the self-oscillation process. For example, if the MEDSAH monomer is replaced with poly(acrylic acid) (PAA) to remove -SO$_3^-$ and N$^+$ groups, testing results show only DC outputs as shown in Fig. 3d. In another example, -COOH groups are removed by replacing the AA monomer with acrylamide to result in only DC outputs in Fig. 3e. These two counterexamples suggest that the key ingredients and reactions as proposed in the polymer system are indispensable to induce surface potential oscillations for AC outputs of moisture-induced energy harvesters.

Parameters Affecting The Outputs And Application Demonstration

The electrical outputs of moisture-induced energy harvesters have been studied by changing the compositions of P(MEDSAH-co-AA) polymer and the working temperature. Under a background

temperature of 28 °C, the peak short-circuit current density and open-circuit voltage of energy harvesters with the MEDSAH/AA ratios of 1/2, 1/3, and 1/4 are shown in Fig. 4a and the output current curves are shown in **Fig. S9**. In order to reduce the influence of environmental noises, a capacitor (4.7 µF) has been charged by prototype devices with a rectifier and its voltage outputs have been recorded in **Figs. 10a** and **S10b**. It is found that by increasing the MEDSAH/AA ratios, the peak current density and voltage increase from 2 µA/cm^2 and 0.32 V to 2.8 µA/cm^2 and 0.4 V as more protons are released by increasing the -COOH groups in the system. The average current oscillation period, which is related to the reaction kinetics, is found to maintain at around 72 seconds for all tested polymers of different compositions as depicted in Fig. 4b. The simulation results also predict the increase of oscillation amplitude as the AA composition increases (**Fig. S11**). On the other hand, under a MEDSAH/AA ratio of 1/2, the peak short-circuit current density and open-circuit voltage of a prototype energy harvester under 12 °C, 28 °C, and 60 °C are tested as shown in Fig. 4c (more details in **Fig. S10c** and current outputs in **Fig. S12**). When the temperature is lowered to 12 °C, the peak current density and voltage values slightly decrease to 1.9 μA/cm^2 and 0.30 V, while the average oscillation period increases to 97 seconds (**Fig. S12a**). As the working temperature reaches 60 °C, the peak current density and voltage values increase to 2.4 μA/cm^2 and 0.33 V, and the average oscillation period decreases to 57 seconds, as the reaction speed is enhanced at high temperature under more energized states (**Fig. S12b**). This phenomenon of negative correlation between the temperature and oscillation period is also predicted by simulations shown in **Fig. S13**.

The performances of the prototype moisture-enabled energy harvester are shown in Fig. 5. In general, prior works have shown that moisture-induced energy harvesters can generate DC outputs. Here, the autonomous surface potential oscillations can be used in prototype energy harvesters to produce alternating current (AC) outputs under relatively high moisture levels in various external environment. For example, testing results show an operation time of more than 15000 seconds (about 4 hours), with an output energy density of 16.8 mJ/cm^2. This long operation time enables long and sustainable energy outputs driven by a relatively constant moisture source as the green energy supply.

A simple strategy to improve the output voltage of the energy harvester is to connect devices in series. As shown in Fig. 6a, the outputs of five devices (MEDSAH/AA ratio of 1/4) are rectified and connected in series to reach a 2-Volts output, which is high enough to light up an LCD (**Movie S2**). A practical application demonstration is implemented in Fig. 6b by connecting five devices in series on the wall of a bathroom full of moisture during the shower time to light up an LCD. This is a direct validation that the moisture-enabled energy harvester can be used in naturally-produced high moisture environment to produce electrical energy in a sustainable manner.

Conclusion

In summary, a surface potential oscillation phenomenon in moisture-induced P(MEDSAH-co-AA) structure has been characterized and an AC energy harvester has been demonstrated. Chemical reactions

responsible for the autonomous potential oscillation behavior are analyzed, modelled by kinetic simulations, and validated by KPFM tests. A prototype energy harvester has a measured peak short-circuit current density of 2.8 µA/cm^2 and peak open-circuit voltage of 0.4 V with a long operation time up to 15000 seconds in moisture-rich environment with an energy density of 16.8 mJ/cm^2. As a practical application demo, an LCD is successfully lit up by connecting five energy harvesters in series to reach the output voltage of 2 Volts.

Experimental Section

Polymer synthesis process

All chemicals are bought from Sigma-Aldrich and used without further treatment. First, the monomers and the initiator are weighted according to the designed ratio and solved in DI water with the weight ratio equals to 63 wt%. The initiator, APS, is 2 mol% compared with monomers. After fully mixed, the solution is poured into a plastic petri dish and heated at 50 °C for 24 h.

Device fabrication

After the polymer synthesis process, an individual specimen is cut into 2 × 2 cm^2 pieces. A polyimide (PI) film of 20µ m in thickness is sputtered with 100-nm-thick Au can cut into electrodes. The top electrode has 25 mechanically punched holes (diameter of 2 mm) to allow the exposure to moistures. Finally, the electrodes are adhered to the polymer structure to complete the device fabrication.

Electric signal measurement

The electrical current is measured via a current amplifier (SR570), and the output voltage is measured by a Data Acquisition system (DAQ, National Instruments).

Characterizations:

(1) EDX tests are performed on a Scanning Electron Microscope (Hitachi 2460 with KEVEX) at 40 keV and the dwelling time is 5 μs.

(2) ATR-FT-IR spectroscopy of dry and wet samples are performed on a Bruker ALPHA Platinum ATR-FT-IR spectrometer equipped with a single reflection diamond ATR module in the ambient atmosphere.

(3) The surface potential is measured using KPFM on an MFP-3D atomic force microscopy (AFM; Asylum Research, Santa Barbara, CA) with Ti/Pt-coated AC250TM-R3 (Oxford Instruments) AFM tip with a radius of ~ 28 nm, spring constant of ~ 2 N/m, and resonant frequency of ~ 70 kHz. All measurements are performed at atmospheric pressure, ~ 20 °C, ~ 40% of relative humidity.
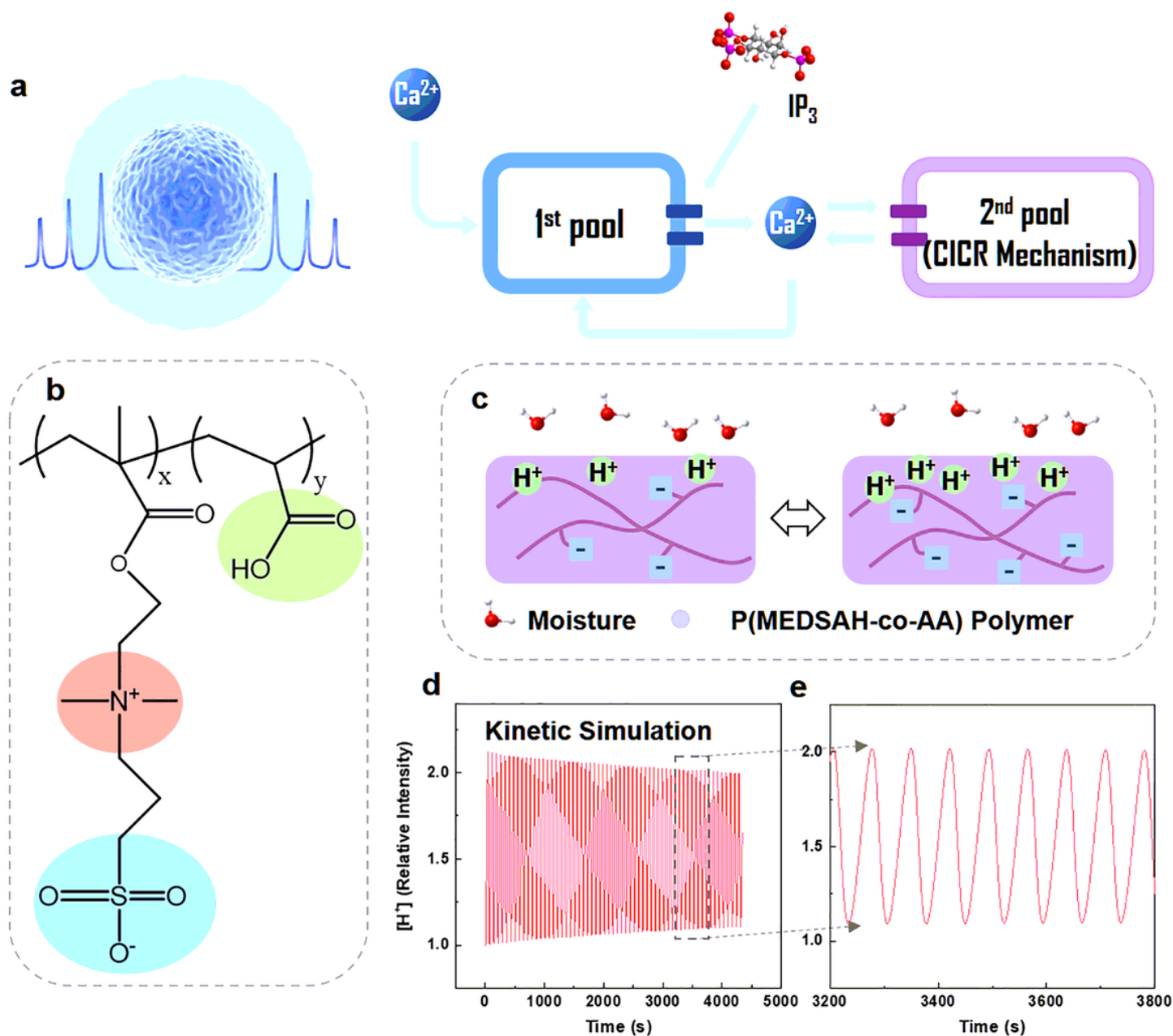
Declarations

Acknowledgements

References

1. Liu, G. *et al.* An ecological risk assessment of heavy metal pollution of the agricultural ecosystem near a lead-acid battery factory. *Ecol. Indic.* **47**, 210–218 (2014).

2. Nandakumar, D. K., Vaghasiya, J. V., Yang, L., Zhang, Y. & Tan, S. C. A solar cell that breathes in moisture for energy generation. *Nano Energy* 104263 (2019).

3. Chang, X. *et al.* Carbon-based CsPbBr 3 perovskite solar cells: all-ambient processes and high thermal stability. *ACS Appl. Mater. Inter.* **8**, 33649–33655 (2016).

4. Yi, F., Zhang, Z., Kang, Z., Liao, Q. & Zhang, Y. Recent advances in triboelectric nanogenerator-based health monitoring. *Adv. Funct. Mater.* 1808849 (2019).

5. Oh, H. *et al.* Highly conductive ferroelectric cellulose composite papers for efficient triboelectric nanogenerators. *Adv. Funct. Mater.* 1904066 (2019).

6. Zhao, F., Liang, Y., Cheng, H., Jiang, L. & Qu, L. Highly efficient moisture-enabled electricity generation from graphene oxide frameworks. *Energy Environ. Sci.* **9**, 912–916 (2016).

7. Xu, T. *et al.* Electric power generation through the direct interaction of pristine graphene-oxide with water molecules. *Small* **14**, 1704473 (2018).

8. Liang, Y. *et al.* Electric power generation via asymmetric moisturizing of graphene oxide for flexible, printable and portable electronics. *Energy Environ. Sci.* **11**, 1730 (2018).

9. Cheng, H. *et al.* Spontaneous power source in ambient air of a well-directionally reduced graphene oxide bulk. *Energy Environ. Sci* **11**, 2839 (2018).

10. Liu, J. *et al.* Moisture-enabled electricity generation from gradient polyoxometalates-modified sponge-like graphene oxide monolith. *J. Mater. Sci.* **54**, 4831–4841 (2019).

11. Huang, Y. *et al.* Interface-mediated hygroelectric generator with an output voltage approaching 1.5 volts. *Nat. Commun.* **9**, 4166 (2018).

12. Li, Q. *et al.* Flexible carbon dots composite paper for electricity generation from water vapor absorption. *J. Mater. Chem. A* **6**, 10639–10643 (2018).

13. Shao, C. *et al.* Wearable fiberform hygroelectric generator. *Nano Energy* **53**, 698–705 (2018).

14. Liu, K. *et al.* Induced potential in porous carbon films through water vapor absorption. *Angew. Chemie* **128**, 8135–8139 (2016).

15. Xu, T. *et al.* An efficient polymer moist-electric generator. *Energy Environ. Sci.* **12**, 972–928 (2019).

16. Nie, X. *et al.* Gradient doped polymer nanowire for moistelectric nanogenerator. *Nano Energy* **46**, 297–304 (2018).

17. Luo, Z., Liu, C. & Fan, S. A moisture induced self-charging device for energy harvesting and storage. *Nano Energy* **60**, 371–376 (2019).

18. Tulachan, B. *et al.* Electricity from the silk cocoon membrane. *Sci. Rep.* **4**, 5434 (2014).

19. Zhen, Z. *et al.* A non-covalent cation-π interaction-based humidity-driven electric nanogenerator prepared with salt decorated wrinkled graphene. *Nano Energy* **62**, 189–196 (2019).

20. Shen, D. *et al.* Self-powered wearable electronics based on moisture enabled electricity generation. *Adv. Mater.* **30**, 1705925 (2018).

21. Gwang Yun, T. *et al.* Transpiration driven electrokinetic power generator. *ACS Nano* **13**, 12703–12709 (2019).

22. Li, M. *et al.* Biological Nanofibrous Generator for Electricity Harvest from Moist Air Flow. *Adv. Funct. Mater.* **29**, 1901798 (2019).

23. Liu, X. *et al.* Power generation from ambient humidity using protein nanowires. *Nature* **578**, 550–554 (2020).

24. Yoshida, R. *et al.* Self-oscillation of polymer chains with rhythmical soluble-insoluble changes. *J. Am. Chem. Soc.* **124**, 8095–8098 (2002).

25. He, T. *et al.* Self-sustainable wearable textile nano-energy nano-system (NENS) for next-generation healthcare applications. *Adv. Sci.* **6**, 1901437 (2019).

26. Namli, O. C. & Taya, M. Design of Piezo-SMA Composite for thermal energy harvester under fluctuating temperature. *J. Appl. Mech.* **78**, 031001 (2011).

27. Adiyan, U. *et al.* Shape memory polymer resonators as highly sensitive uncooled infrared detectors. *Nat. Commun.* **10**, 4518 (2019).

28. Kanik, M. *et al.* Strain-programmable fiber-based artificial muscle. *Science* **365**, 145–150 (2019).

29. Kuksenok, O. *et al.* Modeling chemoresponsive polymer gels. *Annu. Rev. Chem. Biomol. Eng.* **5**, 35–54 (2014).

30. Homma, K. *et al.* Stable and prolonged autonomous oscillation in a self-oscillating polymer brush prepared on a porous glass substrate. *Langmuir* **35**, 9794–9801 (2019).

31. Yoshida, R. & Ueki, T. Evolution of self-oscillating polymer gels as autonomous polymer systems. *NPG Asia Mater.* **6**, e107 (2014).

32. Yashin, V. V. & Balazs, A. C. Pattern formation and shape changes in self-oscillating polymer gels. *Science* **314**, 798–801 (2006).

33. Zhou, H. *et al.* A modular approach to self-oscillating polymer systems driven by the Belousov-Zhabotinsky reaction. *RSC Adv.* **5**, 13555 (2015).
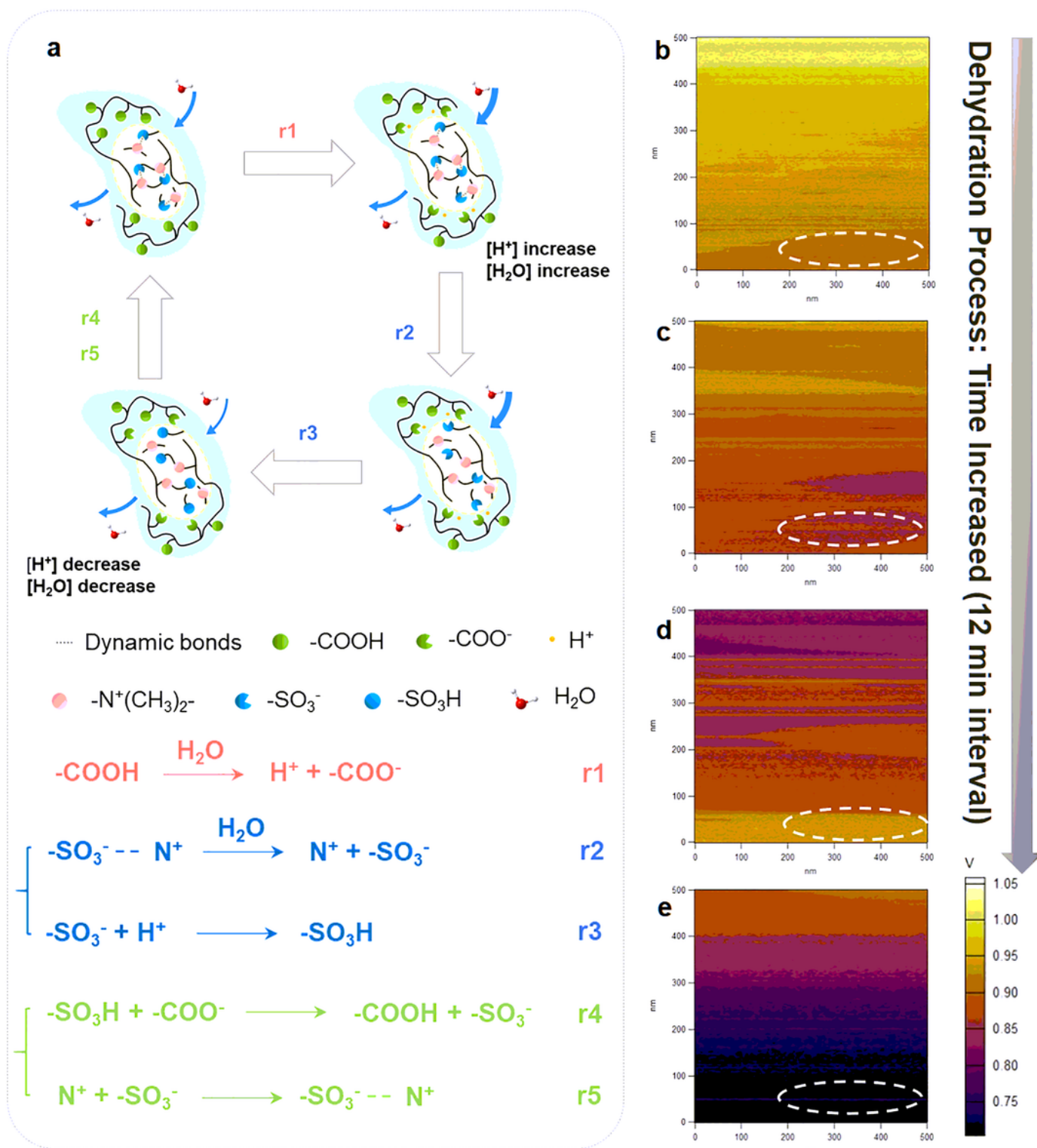
34. Kumar, K. *et al.* A chaotic self-oscillating sunlight-driven polymer actuator. *Nat. Commun.* **7**, 11975 (2016).

35. Soo Kim, Y. *et al.* Receent developments in self-oscillating polymeric systems as smart materials: from polymers to bulk hydrogels. *Mater. Horizons* **4**, 54 (2017).

36. Tamate, R. *et al.* Recent advances in self-oscillating polymer material systems. *Chem. Rec.* 1852–1867 (2016).

37. Arimura, T. & Mukai, M. A self-oscillating gel actuator driven by ferroin. *Chem. Commun.* **50**, 5863 (2014).

38. Takeoka, Y., Watanabe, M. & Yoshida, R. Self-sustaining peristaltic motion on the surface of a porous gel. *J. Am. Chem. Soc.* **125**, 13320–13321 (2003).

Figures

Figure 1

Bio-inspired design strategy. (a) A schematic diagram illustrating the mechanism of Ca2+ concentration oscillations in a living cell. (b) The chemical structure of the as-synthesized P(MEDSAH-co-AA) polymer. (c) A schematic diagram showing the mechanism of the surface potential oscillation with exposure to moistures on the surface of P(MEDSAH-co-AA). (d) Kinetic simulation results of H+ concentration over time due to the transportations of N+, -SO3-, and -COOH groups. (e) Enlarged view of the kinetic simulation result.

Figure 2

A model for the surface potential oscillation induced by moistures. (a) A schematic diagram of the proton transportation via the functional groups of N+, -SO3-, and -COOH in P(MEDSAH-co-AA) with related chemical reaction equations: (r1) proton generations, (r2, r3) proton reduction, and (r4, r5) intermediate interactions on functional groups. (b-e) Kelvin probe force microscopy (KPFM) for surface potential oscillation results at the same surface location of a prototype polymer during the moisture activation and

dehydration process. Each test is taken for about 12 minutes to complete the area-scanning process and the white elliptical area highlights surface potential oscillations. Other areas have also through the surface potential oscillations with slightly different surface potential values.
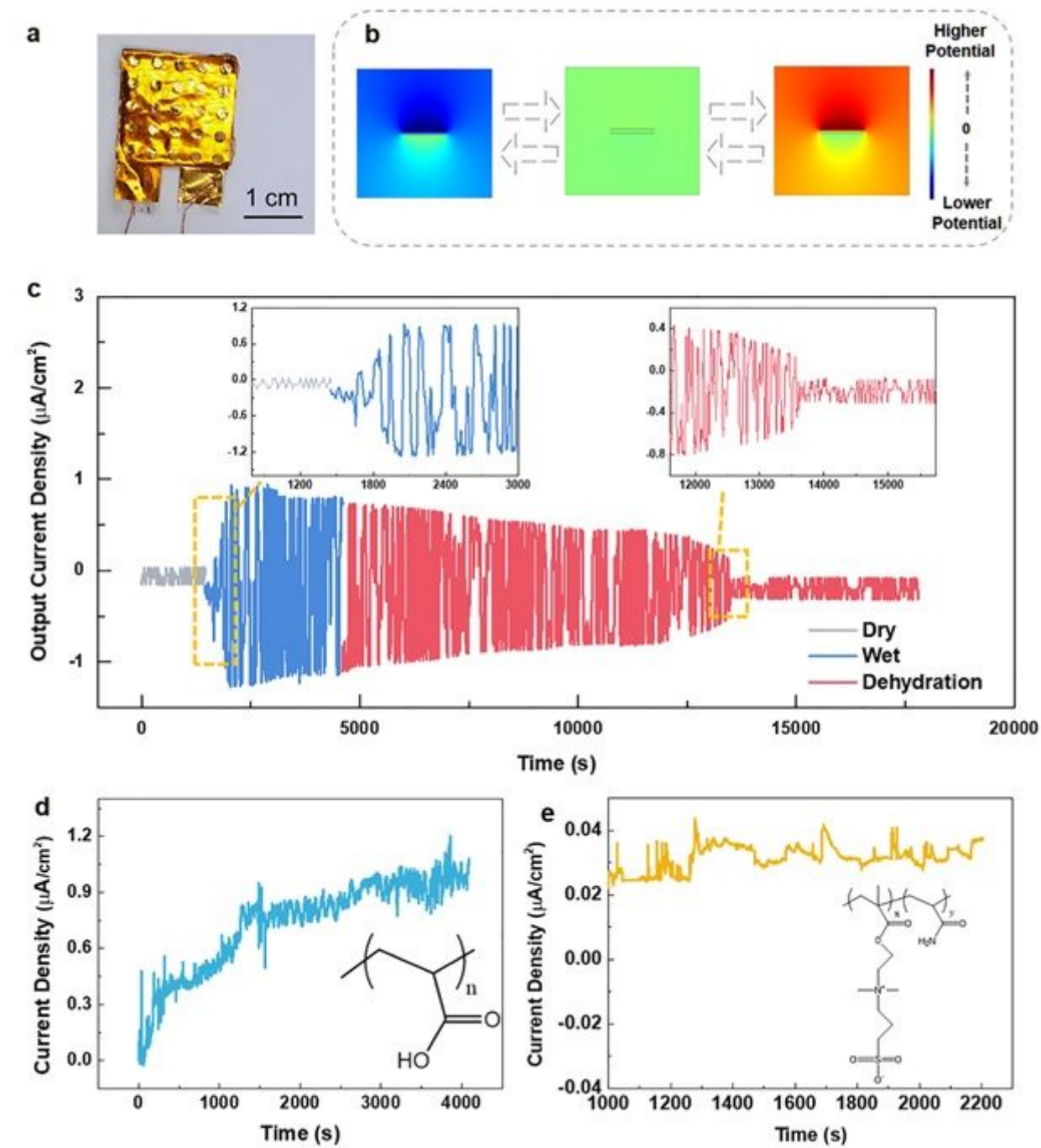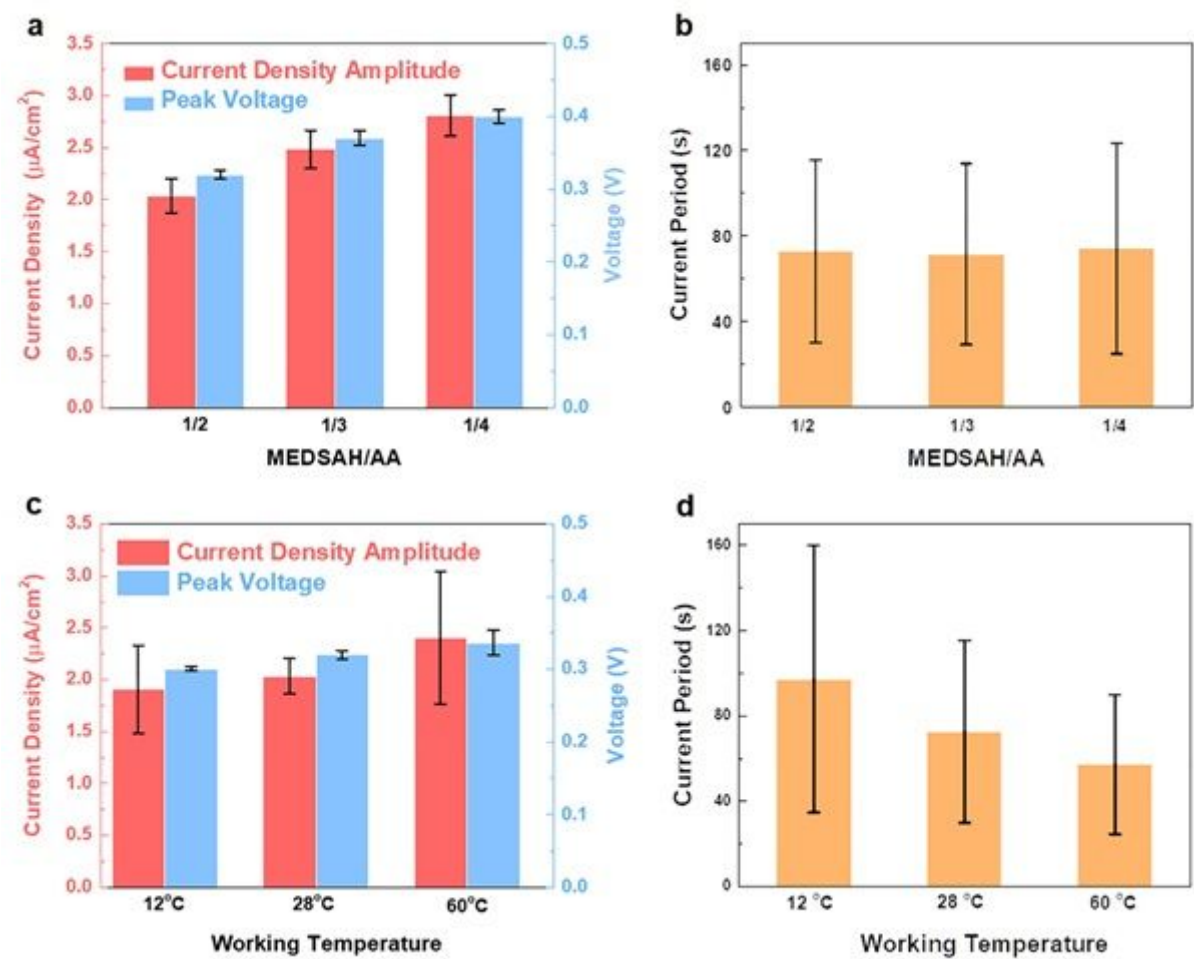

Figure 3

Energy harvester based on surface potential oscillations. (a) An optical photo of a fabricated energy harvester. (b) COMSOL simulation results showing the surface potential oscillation of an energy harvester versus time. (c) Output short-circuit current density versus time of a prototype energy harvester before the introduction of the moisture (grey color), after the moisture wetting process by a humidifier (blue color), and the dehydration process after removing the humidifier (red color). Insets show enlarged views for the

wetting (upper left) and dehydration (upper right) processes. (d) An example of replacing MEDSAH monomer with PAA to remove the SO3- and N+ groups in the polymer, which stops the autonomous oscillations to result in DC electrical outputs. (e) In another example, the AA monomer is replaced with acrylamide to remove the -COOH groups and only DC outputs are observed.

Figure 4

Electrical output characterizations for moisture-induced energy harvesters with different monomer ratios and under different temperature environments. (a) Peak short-circuit current density and open-circuit voltage for energy harvesters with the MEDSAH/AA ratios of 1/2, 1/3, and 1/4, under 28oC. (b) Average oscillation periods of energy harvesters with MEDSAH/AA ratios of 1/2, 1/3, and 1/4, under 28 oC. (c) Peak short-circuit current density and open-circuit voltage of energy harvesters under temperatures of 12, 28, and 60oC, respectively. (d) Average oscillation periods of energy harvesters under temperatures of 12, 28, and 60 oC, respectively.
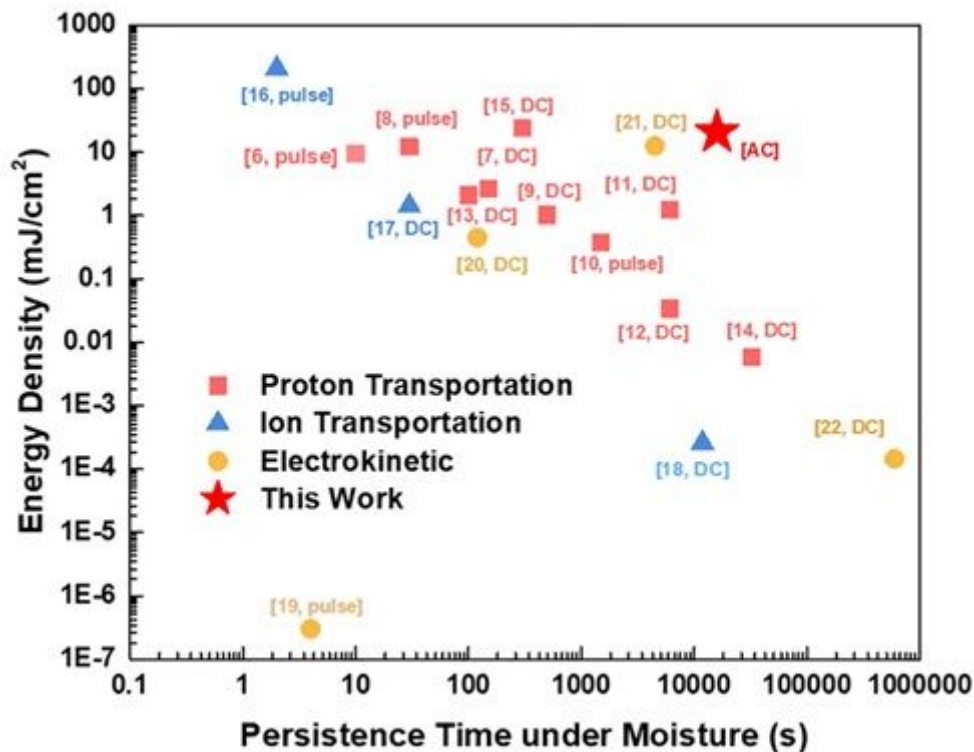
Figure 5

Comparison moisture-induced electric generators based on artificial materials in the operation time and energy density. This work has long persistence time and high energy density among moisture-based energy harvester, and these two parameters could be further improved by using other materials based on similar self-oscillation mechanisms.
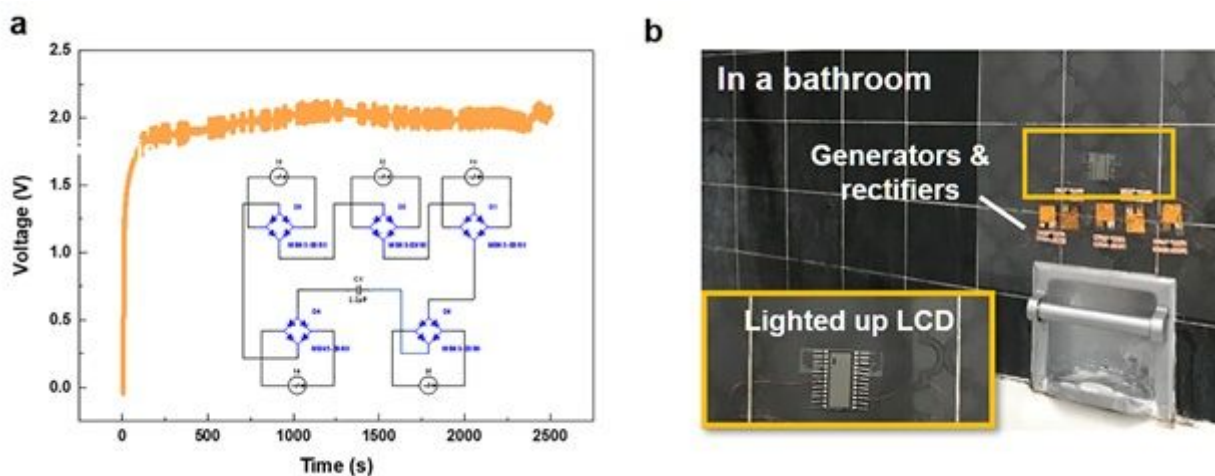

Figure 6

Demonstrations of moisture-induced energy harvesters. (a) Rectified output voltage vs. time by five devices connected in series. Inset: the detailed circuit. (b) Lighting up an LCD in a bathroom with moisture during the shower time. The inset shows the enlarged view.

Supplementary Files

This is a list of supplementary files associated with this preprint. Click to download.

- SupplementaryMaterialsNC.docx
- MovieS1.avi
- MovieS2.avi